

Growth by random walker sampling and scaling of the dielectric breakdown modelEllák Somfai,^{*} Nicholas R. Gould,[†] and Robin C. Ball[‡]*Department of Physics, University of Warwick, Coventry CV4 7AL, United Kingdom*Jason P. DeVita[§] and Leonard M. Sander^{||}*Michigan Center for Theoretical Physics, Department of Physics, University of Michigan, Ann Arbor, Michigan 48109-1120, USA*

(Received 18 March 2004; published 17 November 2004)

Random walkers absorbing on a boundary sample the harmonic measure linearly and independently: we discuss how the recurrence times between impacts enable nonlinear moments of the measure to be estimated. From this we derive a technique to simulate dielectric breakdown model growth, which is governed nonlinearly by the harmonic measure. For diffusion-limited aggregation, recurrence times are shown to be accurate and effective in probing the multifractal growth measure in its active region. For the dielectric breakdown model our technique grows large clusters efficiently and we are led to significantly revise earlier exponent estimates. Previous results by two conformal mapping techniques were less converged than expected, and in particular a recent theoretical suggestion of superuniversality is firmly refuted.

DOI: 10.1103/PhysRevE.70.051403

PACS number(s): 61.43.Hv

I. INTRODUCTION

The steady-state distribution of random walking particles is governed by Laplace's equation. As a result Witten and Sander's model of diffusion-limited aggregation (DLA) [1], in which a cluster grows by irreversible accretion of dilute diffusing material, has been of double interest: it is readily simulated out to huge cluster sizes [2,3], while at the same time the governance of its growth by Laplace's equation renders it a landmark mathematical challenge to analyze. The connection to a Laplacian field also underpins the breadth of application of the DLA model to problems such as viscous fingering in porous media [4] and electrodeposition [5,6]. This interest has all been abetted by controversy as to whether the distribution of cluster shapes conforms to simple fractal scaling (see [7] and references therein) and interest in the multifractal scaling of the growth measure [8–11].

Physical analogies and the mathematical connections have led to interest in other models where the growth is governed *nonlinearly* by a Laplacian field. In particular Niemeyer, Pietronero, and Wiesmann introduced the family of dielectric breakdown models (DBM's) [12] where

$$v_n \propto |\partial_n \phi|^\eta, \quad \nabla^2 \phi = 0, \quad \phi_{\text{interface}} \approx 0, \quad (1)$$

and η is (for interest) a positive parameter. Interest in this is further prompted by Ball and Somfai's proposal [13,14] that growth proportional to field with nontrivial spatial cutoff maps onto a simple DBM but with $\eta \neq 1$. An important case in point is diffusion-controlled growth which is limited lo-

cally by the capillary energy associated with surface ramifications. Computationally these nonlinear models have been a challenge, as random walkers only directly sample the harmonic measure linearly, realizing only the $\eta=1$ case.

First in this paper we show that random walkers can be exploited to sample nonlinear moments of the harmonic measure. In this way we obtain results for the active portion of the multifractal spectrum of DLA far beyond existing results. The key strength of these methods is that no explicit solving of the Laplace equation is involved.

We then exploit this to establish a method of growing DBM clusters by random walker accretion. This also entails adopting the noise reduction strategies lately introduced in Ref. [15] and enables us to explore the DBM class out to unprecedentedly large clusters. We show that in two dimensions this largely resolves how the exponents of the DBM model depend on η : in particular superuniversality of the tip scaling exponent α is strongly refuted, in favor of a continuous variation of exponents which also confirms the hypothesized upper critical value [16–19] $\eta_c=4$.

Our walker-DBM results are supported by extensive computations using established iterative conformal mapping methods due to Hastings and Levitov (HL) [20] and also by direct integration of the Shraiman-Bensimon equations [21] exploiting the mappings of Ball and Somfai [13,14]. For exponents, all three agree within statistical errors. Below the level of the errors there is a systematic difference between walker-DBM and HL, and separate results for the relative penetration depth suggest that it is the walker-DBM clusters which are more converged to asymptotic behavior. Unlike HL and our Shraiman-Bensimon integrations, the walker-DBM technique is not limited to two dimensions and so the way forward appears open to a full exploration of the DBM class in three dimensions.

II. RANDOM WALKER SAMPLING

We consider first the problem of sampling the harmonic measure of an equipotential surface. The harmonic measure

^{*}Present address: Universiteit Leiden, Instituut-Lorentz, P.O. Box 9506, 2300 RA Leiden, The Netherlands. Electronic address: ellak@lorentz.leidenuniv.nl

[†]Electronic address: N.R.Gould@warwick.ac.uk

[‡]Electronic address: r.c.ball@warwick.ac.uk

[§]Electronic address: jdevita@umich.edu

^{||}Electronic address: lsander@umich.edu

is given on the surface by $d\mu/ds = \partial\phi/\partial n$ where outside the surface the scalar field ϕ obeys a Poisson equation $-\nabla^2\phi = S(x)$ with $S(x)$ the source density; typically, we will be interested in cases where the source is concentrated at points, particularly ∞ . We can sample this measure by introducing random walkers at the source points and tracing their Brownian trajectories to the point of first encounter with the surface, whereupon any given walker is discarded. The points of first encounter uniformly sample the measure μ .

By firing a large enough sample of random walkers and collecting frequency counts of their hit distribution, one can build up an approximation to the entire harmonic measure. This procedure has been successfully used by Somfai *et al.* [7]. However, such methods are expensive and give differing quality estimates across the support.

Here we focus on recurrence times defined as follows. We first divide the support into (many) small partitions (hereafter termed “sites”) for each of which we aim to estimate the corresponding hit probability μ . We then fire (independent) walkers sequentially at the surface, and when each walker hits, the number of walkers fired since the previous hit on that site we will call the “age” a , and this provides a simple estimate of the hit probability of that site $\mu_1 = 1/a$. This is a standard way to estimate frequency of uncorrelated events, by their recurrence time. The probability distribution of the estimator μ_1 , given the true underlying value μ for that site, is given by simple Poisson statistics as

$$p_1(a|\mu) = \mu e^{-\mu a},$$

assuming that $\mu \ll 1$ so that we can approximate age as a continuous variable. We can generate more reliable estimates by using the age a_k since the k th previous hit, which is distributed according to

$$p_k(a_k|\mu) = \mu e^{-\mu a_k} (\mu a_k)^{k-1} / (k-1)!, \quad (2)$$

in terms of which our estimate is $\mu_k = k/a_k$.

In applications considered below we will be interested in calculating moments of the measure, $M_q = \sum \mu^q$, where the summation is over the sites into which we partitioned the support. This can be interpreted as $M_q = \langle \mu^{q-1} \rangle$ where the average is weighted by the measure μ itself which in turn is sampled by where random walkers hit. At each impact we can use the site age in our estimate for the factors μ^{q-1} , leading to the estimate

$$M_{qk} = A(k, q) \langle (a_k/k)^{1-q} \rangle,$$

where the average is now over all random walkers hitting the surface, we use k th ages, and $A(k, q)$ is a trivial numerical front factor.

Random walkers being cheap, our main concern is when this estimate converges. Using the distribution (2) one can readily check that the integral for M_{qk} converges to M_q provided $k > q-1$, and we use the appropriate prefactor $A(k, q) = [k^{1-q}(k-1)!] / (k-q)!$. Thus we can compute moments of finite degree simply by using high enough order ages. In practice we will see that for problems of interest the most significant limitation comes not at high q but rather at

highly negative q , for which random walkers give an inefficient sample of the relevant parts of the measure.

III. MOMENTS UNDER GROWTH

The simple ideas above become rather useful when extended to compute moments of the measure as a surface grows. The harmonic measure of diffusion-limited aggregation provides a well-studied (but not entirely resolved) test case. For a cluster of N added particles the conventional multifractal scaling would lead to $M_q \sim N^{-\tau(q)/D}$, where D is the fractal dimension relating radius R to N through $N \sim R^D$. Summing these moments over N with weight N^{t-1} gives us a partition function $Z(q, t)$ which we can estimate (ignoring numerical prefactors) as

$$Z(q, t, N) = \sum_{n=1}^N a^{1-q} n^{t-1},$$

where the sum is now over the particles used to grow the cluster and the corresponding ages of the sites where they hit. Following the spirit of how Halsey *et al.* [22] generalized the identification of multifractal spectrum, we can now identify that $\tau(q)/D$ separates the values $t < \tau(q)/D$ for which $Z(q, t, N) \rightarrow \infty$ as $N \rightarrow \infty$ from the values $t > \tau(q)/D$ for which $Z(q, t, N) \rightarrow 0$.

The above definition does not restrict the behavior of $Z(q, t, N)$ on the locus $t = \tau(q)/D$ but the simple expectation is of a logarithmic divergence with N . Then a numerical strategy is to choose t such that

$$Z(q, t, N) - Z(q, t, \epsilon N) = \sum_{n=\epsilon N+1}^N a^{1-q} n^{t-1}$$

becomes independent of N as N becomes large with fixed ϵ .

To obtain results at $q \geq 2$ we have to use higher-order ages. The first-order age is naturally thought of as the age of the parent to a given new site and a corresponding estimate of a_2 is given by the age of its grandparent (the parent of its parent) and so on. It is of course a concern that the more such generations one looks back for the age, the more the cluster geometry will have evolved in the meantime: we will see that overall cluster screening cuts in below a threshold value of q in a well understood way. To alleviate the worry above threshold we have studied noise-reduced clusters where each particle deposited advances the local geometry by only a small fraction A of one notional particle size, so that we can be confident that the local geometry does not evolve significantly on looking back of order $1/A$ generations.

Figure 1 shows the moment spectrum $\tau(q)$ resulting from imposing the condition $Z(q, t, N) - Z(q, t, \epsilon N) = Z(q, t, \epsilon^2 N) - Z(q, t, \epsilon^3 N)$ on a *single* off-lattice DLA cluster. As expected from our discussion in Sec. II, the results using ages of order k break away at $q = k+1$. An important check is given by the measured value $\tau(3)/D = 1.01$ compared to the prediction of unity from the electrostatic scaling law [23].

For more definitive results we have studied a sample of 10 clusters out to $N = 10^7$ using $A = 0.1$. Even allowing for the noise reduction, which means that of order $1/A = 10$ particles

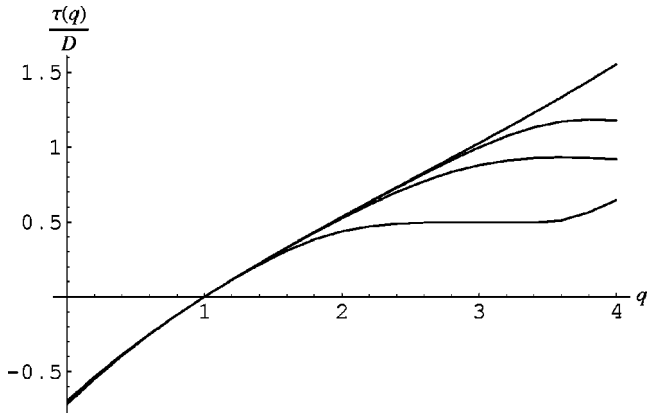


FIG. 1. The moment spectrum $\tau(q)$ of the harmonic measure obtained over the growth of a single DLA cluster by imposing the condition $Z(q, t, N) - Z(q, t, N/4) = Z(q, t, N/4) - Z(q, t, N/16)$ to yield $t = \tau(q)/D$. The respective curves used ages of order $k = 1, 2, 4, 8$ and can be seen to break away around $q = k + 1$ as expected from our discussion in Sec. II. Note also the close agreement with the electrostatic scaling law [23] that $\tau(3)/D = 1$. These results come from a single off-lattice DLA cluster of $N = 10^6$ particles grown with noise reduction factor [15] $A = 0.1$.

were deposited per local unit of advance in the growth, it is unprecedented to probe the harmonic measure out to such large scales. Because of the volume of age data, it was cumbersome to seek stationarity of $Z(q, t, N) - Z(q, t, \epsilon N)$ and instead we extracted $t(q)$ from the simple scaling expectation that $Z(q, t', N) - Z(q, t', \epsilon N) \propto N^{t' - t(q)}$ where we simply chose t' to assure reasonably uniform weighting of the data. We then took $\tau(q) = Dt(q)$ using $D = 1.71$, where any error in this value is not significant to the accuracy of $t(q)$. The resulting $f(\alpha)$ spectrum is shown in Fig. 2 for ages of order $k = 1, 3, 9, 27$ and compared to one earlier report of the $f(\alpha)$ spectrum

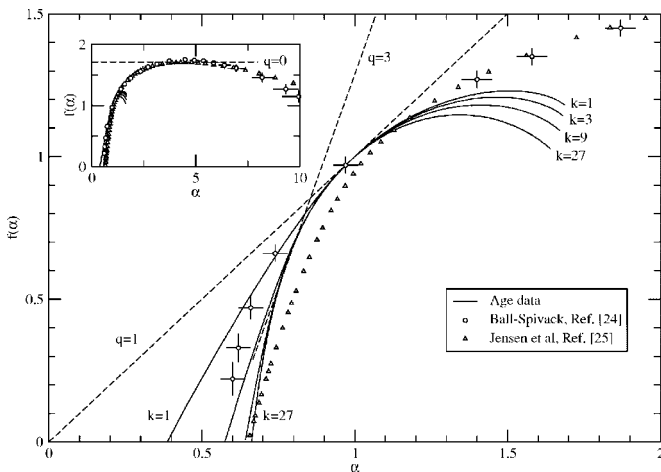


FIG. 2. Multifractal spectrum of (the harmonic measure of) DLA obtained using ages of order $k = 1, 3, 9, 27$. Also shown are earlier results from Ball and Spivack [24] and Jensen *et al.* [25]. Note how much better the present data agree with the tangent lines representing Halsey's electrostatic scaling law (for $q = 3$) and Makarov's theorem (for $q = 1$). The inset shows how the older data extend to higher α , which our method cannot probe.

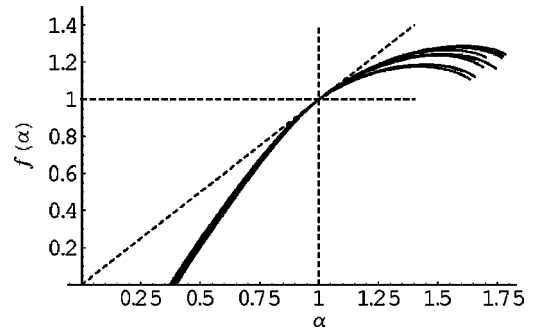


FIG. 3. Size dependence of the $f(\alpha)$ spectrum of DLA, obtained using first-order ages and clusters grown per Fig. 2 to different sizes. In the vicinity $\alpha \leq D$ the curves systematically rise with the range of N used, in support of our claim that the age method ultimately probes all the way to $\alpha = D$. The curves are based on the slope of $\ln Z(q, 0, N)$ vs $\ln N$ across successive factors of $\sqrt{10}$ in N up to $N = 10^7$ (topmost curve).

which is distinguished by carrying full error bars [24] and one more recent spectrum [25] which claimed better convergence than all previous.

The success of our data lies in the region $q \geq 1$ corresponding to $\alpha \leq 1$, where it passes two important tests by meeting the (dashed) tangent lines corresponding to Makarov's theorem [26] at $q = 1$ and (for the higher k as appropriate) Halsey's electrostatic scaling law [23] at $q = 3$, and in these respects it clearly improves on the earlier published data.

A significant limitation of the $f(\alpha)$ spectrum obtained is that it substantially undershoots at large α , but this is qualitatively consistent with expectations. It is obvious that we cannot expect to probe probabilities to hit a site which are smaller than $1/N$ as these are unlikely to be sampled by the N walkers used to grow the cluster. Thus we certainly cannot probe the spectrum for $\alpha > D$.

A more careful argument suggests that in principle we should (in the limit of large enough N) be able to probe all the way up to $\alpha = D$, as follows. Consider a typical site X "born" with hit probability $R^{-\alpha}$, $\alpha < D$. It is expected that the probability for growth within distance r of this point varies as $p(r) \approx (r/R)^\alpha$, and when this vicinity has received r^D walkers the local structure up to length scale r will have been completely regrown. This requires a number of walkers added to the cluster given by $\delta N (r/R)^\alpha \approx r^D$ leading to $\delta N \approx R^\alpha r^{D-\alpha}$. The argument is consistent for $\alpha < D$ because it shows that for length scales larger than r the regrowth threshold will not have been met, validating our retention of the hit probability $p(r) \approx (r/R)^\alpha$. From the point of view of site X significant reorganization of the cluster happens first on the smallest scales and requires $\delta N \approx R^\alpha$, by which point we can expect to have hit site X itself with nonzero probability. For $\alpha > D$ the scenario is of screening being dominated by distant growth and hitting the site is unlikely. A more detailed discussion of the screening dynamics is given by Ball and Blunt [9].

Figure 3 shows how the $f(\alpha)$ spectrum from first-order ages develops as a function of size up to $N = 10^7$. As expected the spectrum builds up on the right-hand side (RHS) as we

increase N consistent with our expectation that ultimately we can probe as far as $\alpha=D$. Quantitatively the convergence is poor beyond about $\alpha \approx 1.5$.

IV. DIELECTRIC BREAKDOWN MODEL

A. Random walker model

Niemeyer, Pietronero, and Wiesmann [12] introduced the generalization of diffusion-controlled growth in which the local advance velocity is set by μ^η . In this model $\eta=1$ corresponds to DLA, while growth with higher values of η was proposed to model the evolution of dielectric breakdown patterns. More recently it has been argued by two of us [13,14] that nontrivial values of η can also be induced when mapping between different types of ultraviolet cutoff, even when the underlying growth is strictly proportional to flux. The computational challenge of the DBM is that random walkers sample the harmonic measure proportional to μ , so for $\eta \neq 1$ an explicit calculation of the measure appears to be required. Relaxation methods [8,19] and more recently (for two dimensions) conformal mapping techniques [17] have been used, but the resulting computations are dramatically more expensive than for simple DLA simulation.

We propose that the following random walker growth model is equivalent to the DBM. We fire random walkers at the cluster, whose first encounter linearly samples μ . At each encounter we use the k th-order age of the site hit to give the estimate $\mu_k = k/a_k$ and accordingly advance the growth locally by an amount proportional to $\delta m = A a_k^{1-\eta}$, which is interpreted as the mass added to the cluster. There are two clear constraints: The first is that the local advance must converge in the mean, $\langle a_k^{1-\eta} \rangle_\mu \propto \mu^{\eta-1}$, requiring that $k > \eta - 1$. The second is that we desire that the k th-order ages should look back no further than a particle size, so individual advance steps should be bounded by $1/k$. Naively this requires $A < 1/k$ for $\eta > 1$ and $A < N^{\eta-1}$ for $\eta < 1$, where N is the total number of walkers, but we will discuss below how we can greatly improve on these constraints by adjusting A dynamically.

B. DBM with optimal growth steps

We now consider allowing the growth step prefactors A to vary as the growth proceeds. It is convenient to interpret $A = \delta Q$ as the charge borne by each walker adding to the growth, and the growth is governed by the local normal advance rate $(\partial r / \partial Q)_n = \mu^\eta$ where Q is the cumulative charge added. It was noted by two of us [14] that if we characterize the extremal tips of the growth as having $\mu_{\text{tip}} \approx R^{-\alpha_{\text{tip}}}$, then the growth law at the tips trivially leads to $Q \approx R^{1+\eta\alpha_{\text{tip}}}$ as a generalization of a standard relation for the fractal dimension of DLA, and less trivially it is expected that $1 + \eta\alpha_{\text{tip}} = \tau(2 + \eta)$ which we will use below to render some expressions less cumbersome. Within all this framework we are now free to choose the charge increments per walker δQ to vary systematically with growth of a cluster (but not biased by where each particular walker hits), with the corresponding mass increments given by $\delta m = \delta Q a_k^{1-\eta}$.

We focus on the case $\eta > 1$ for which the concern lies with anomalously low ages which would give large growth

steps. At given $\mu = R^{-\alpha}$, the probability that a single sampling of the k th age is less than a_k can be found from Eq. (2) and varies as $(R^{-\alpha} a_k)^k$ for $\mu a_k \ll 1$. If we grow the cluster by a significant fraction of its size, then the number of walkers sampling this distribution is given by $(Q / \delta Q) R^{f(\alpha) - \alpha}$ where the first factor is the total number of walkers added and the second is the probability of one walker landing on a site with $\mu \approx R^{-\alpha}$. Therefore the number of times ages below a_k are expected to be sampled is given by

$$\max_{\alpha} [Q / \delta Q R^{f(\alpha) - \alpha} (R^{-\alpha} a_k)^k], \quad (3)$$

where we have taken the maximally contributing value of α . To find the smallest likely value of a_k we then set this expression to unity. Maximizing the α dependence gives $\max_{\alpha} [R^{f(\alpha) - \alpha} R^{-k\alpha}] \approx R^{-\tau(k+1)}$ and it is convenient to similarly substitute $Q \approx R^{\tau(2+\eta)}$, leading to expected minimum age given by

$$\min\{a_k\} \approx (R^{\tau(k+1) - \tau(2+\eta)} \delta Q)^{1/k}. \quad (4a)$$

The above calculation is valid when it yields an increasing function of R ; otherwise, the scaling assumption in Eq. (3) does not hold, and we have

$$\min\{a_k\} = 1. \quad (4b)$$

We have tested the predicted minimum age by looking at the extremal ages sampled during DLA cluster growth, where we have $\delta Q = 1$, $\eta = 1$, and $\tau(3) = D$. Figure 4 shows scatter plots of all the ages as a function of cluster growth in terms of $N \approx R^D$, using ages of different orders and comparing with the result above.

We can now exploit the expected minimum age to set an optimal choice of δQ in DBM growth: we substitute $\min\{a_k\}$ into the restriction that the growth steps be suitably limited $\delta m \ll 1$, leading to

$$\delta Q \approx R^{(\eta-1)[\tau(k+1) - \tau(2+\eta)] / (k+1-\eta)}. \quad (5)$$

Given that we are restricted to $k+1 > \eta$, the exponent of R in the expression for δQ increases monotonically with k towards the asymptote $(\eta-1)\alpha_{\text{min}}$ as $k \rightarrow \infty$.

In practice we are inhibited from setting k too large because k -dependent prefactors compete with optimizing the power law for finite R , but taking $k=10$ puts us quite close to the limit. Also, we cannot use Eq. (5) explicitly because the values of $\tau(k+1)$ and $\tau(2+\eta)$ are not known *a priori* for a generic η . Instead, armed with the knowledge that such an asymptotic power law exists, we use the empirical formula $\delta Q = A_0 k^{\eta-2} N^{\beta}$ for which the parameters are chosen such that the constraints are met. For the parameter values of Table I, used in the simulations below, the condition $\delta m < 1$ always holds while the distance looked back by the k th-order age only exceeds one particle diameter a few times per million walkers and never exceeds two particle diameters.

Our algorithm is most competitive for η near 1, including the important region $1 < \eta < 2$ corresponding to surface tension regularization [13,14], where it can generate cluster masses inaccessible by other methods. For too small or large η (particularly $\eta \geq 3$) it becomes less advantageous.

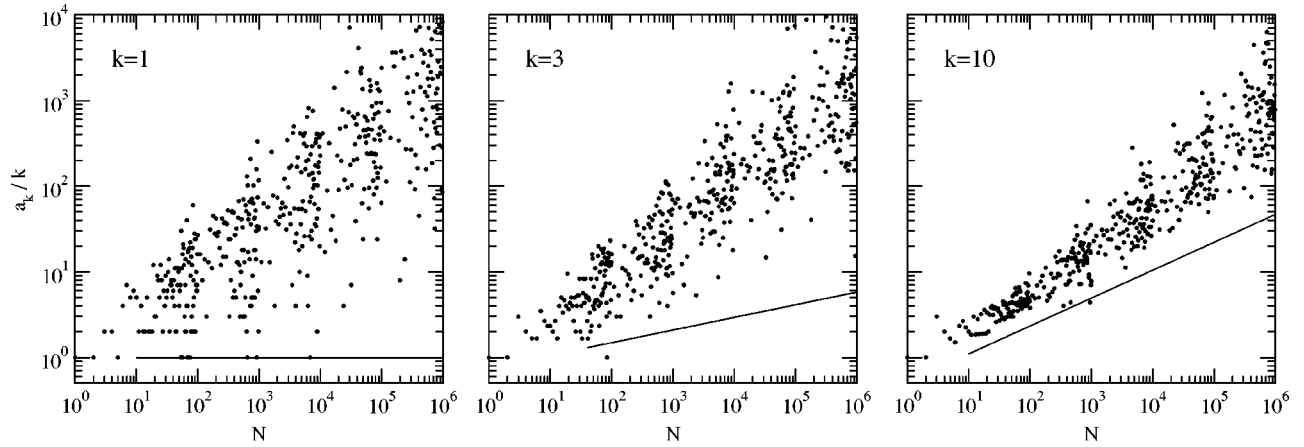


FIG. 4. Scatter plot of the ages of sites hit for DLA: $\eta=1$, $\delta Q=1$. The data points are decimated for large N for clarity. The solid lines correspond to the expected scaling of minimal ages obtained from Eqs. (4a) and (4b); these theoretical estimates appear to be suitably cautious.

In principle for $k \rightarrow \infty$ the number of walkers required to grow a cluster is given by

$$N = \int \frac{dQ}{\delta Q} \approx R^{1+\alpha_{\min}+\eta(\alpha_{\text{tip}}-\alpha_{\min})}.$$

The result is familiar in that for $\eta=1$ it recovers the DLA result (where N is also the cluster mass). There has been recent controversy about the precise value of $\alpha_{\text{tip}}-\alpha_{\min}$ through which our method is explicitly sensitive to η [10], although certainly this difference is very small at $\eta=1$, where $0 \leq \alpha_{\text{tip}}-\alpha_{\min} \leq 0.03 \pm 0.005$; see Fig. 5.

C. Numerical results

Figure 6 shows “snapshots” of DBM clusters grown at different η using the random walker method.

As a test of the walker-DBM method, we compared the relative penetration depth (the growth zone width, normalized by the average deposition radius) with measurements on clusters grown by the more established HL method, for $\eta=2$. The asymptotic behavior of the penetration depth can be considered a sensitive measurement, as for DLA it caused considerable controversy in the past. As seen in Fig. 7, both methods converge to the same asymptotic value of the relative penetration depth, and of the two, the walker-DBM method converges slightly faster. This can be understood in terms of the higher effective noise reduction levels.

To probe the scaling, we measured the tip scaling exponent α_{tip} and the fractal dimension D for several values of η .

TABLE I. Numerical values of the parameters used to grow walker-DBM clusters. The local growth is $\delta m = (A_0/k)N^\beta(a_k/k)^{1-\eta}$.

η	k	A_0	β
0.5	1	0.8	-0.45
1.5	10	0.85	0.138
2	10	0.8	0.234
3	10	0.85	0.32

In Fig. 8 we compare these results with measurements obtained with different methods: HL and by integrating the Shraiman-Bensimon equation, the latter described in more detail in the next section. The data agree within the stated uncertainties, showing a smooth monotonic transition between the extremes $\eta=0$ and $\eta \gtrsim \eta_c$, while below the level of significance point by point one can see some differences. One difference is that for HL, α_{tip} shows very little variation at $1 \leq \eta \leq 2$ (seemingly agreeing with an earlier prediction [13,14]), while the walker-DBM method does not show this feature. Another difference is that for high η the walker-DBM method yields lower values for both α_{tip} and D than HL. Although for the walker-DBM method it was not practical to obtain values for $\eta > 3$, its extrapolation is more consistent with $\eta_c=4$.

V. SHRAIMAN-BENSIMON EQUATION

Shraiman and Bensimon observed [21] that for DLA in two dimensions the evolution of the complex potential reduces to a nonlocal problem in one space dimension (plus time). This is based on the cluster boundary $z(\theta)$ expressed as a complex function of the imaginary part θ of the complex potential, corresponding to cumulative harmonic measure or, more loosely, charge. In Refs. [13,14] we adapted this to the DBM class, arguing that changing from a fixed cutoff scale in physical space to a fixed cutoff in charge space could be offset by adjustment of the DBM parameter from η_0 to $\eta_1 = \alpha\eta_0$. Then, in terms of

$$(-i\partial z/\partial\theta)^{-(1+\eta_1)/2} = \psi(\theta, t) = 1 + \sum_{k=1}^K \psi_k(t) e^{-ik\theta},$$

the dynamics for DBM growth along a channel of width 2π with periodic boundary conditions reduces to

$$\frac{d}{dt} \psi_k = -k\psi_k \sum_{m=0}^K \psi_m \overline{\psi_m} + \sum_{j=1}^k \sum_{m=0}^{K-j} [(3+\eta_1)j-2k] \psi_{k-j} \psi_{j+m} \overline{\psi_m}, \quad (6)$$

with $\psi_0=1$. The fixed bandwidth limit $k \leq K$ corresponds qualitatively to imposing a cutoff of fixed minimal charge on

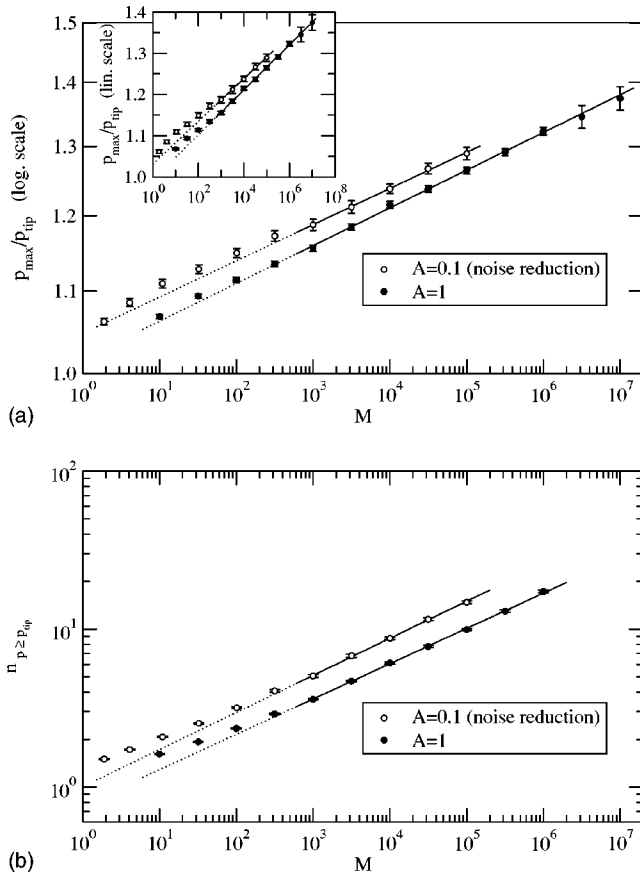


FIG. 5. Study of the highest probability growth sites and the tips of DLA clusters. We launched probe walkers onto a fixed nongrowing cluster and recorded the number of probes landed on each site. This enables us to calculate the growth probability of each site, including the tip (farthest site from the origin). (a) The ratio of the growth probabilities of the highest hit rate site and the tip: it is a slowly increasing function of the cluster mass M . The best fit curve is a power law with a small exponent: $p_{\max}/p_{\text{tip}} \sim M^{(\alpha_{\text{tip}} - \alpha_{\min})/D}$, with $\alpha_{\text{tip}} - \alpha_{\min} = 0.03 \pm 0.005$. However, one cannot entirely exclude logarithmic corrections (see inset); in that case $\alpha_{\text{tip}} = \alpha_{\min}$. (b) The number of sites with higher hit rate than the tip. This scales as a power of the radius R with the fractal dimension of tips as exponent: $n_{p \geq p_{\text{tip}}} \sim R^{f_{\text{tip}}} \sim M^{f_{\text{tip}}/D}$. The exponent is larger, clearly distinct from zero: $f_{\text{tip}} = 0.38 \pm 0.03$. On all plots the two data sets are standard DLA ($A=1$) with 10^4 – 10^5 clusters depending on size and noise-reduced DLA ($A=0.1$) with 4200– 10^4 clusters. The number of probes was set such that the tip of each cluster received 2500 hits. The solid lines are best fit for the data points under them; dotted lines are extensions towards excluded data points.

the growing tips and inevitably means that the most screened regions of the physical growth are not tracked. Scaling arguments lead to the expectation that $\langle \psi_m \psi_m \rangle \propto m^{-1 + \eta_1(1-1/\alpha)}$ for $1 \ll m \ll K$, but give no indication of how wide a range of m is required to see the scaling behavior and hence determine the tip scaling exponent α , and we will see that this is a major issue below.

The trilinear form of the RHS is efficiently evaluated by Fourier methods costing of order $K \ln K$ per time step for the whole system, and in the results presented here we used $K = 1023$ and a simple predictor-corrector time-stepping

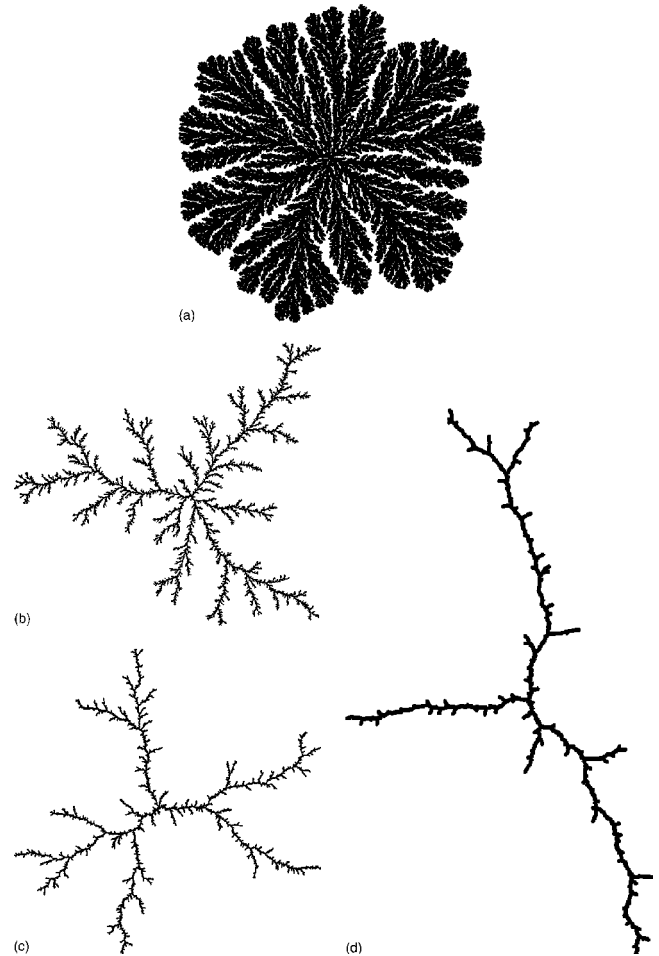


FIG. 6. DBM clusters grown by the new method: (a) $\eta=0.5$, (b) $\eta=1.5$, (c) $\eta=2$, and (d) $\eta=3$. In each case $N=10^6$ random walkers were used.

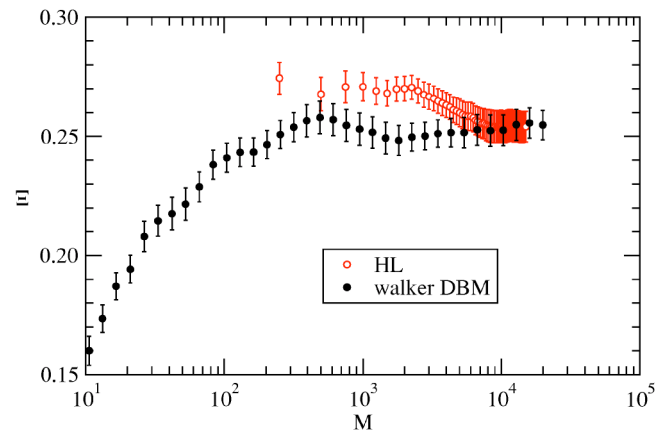


FIG. 7. (Color online) Comparison of the relative penetration depth $\Xi = \sqrt{\langle r^2 \rangle - \langle r \rangle^2} / \langle r \rangle$ for the walker-DBM and HL methods. For each method the penetration depth was measured on 30 DBM clusters, $\eta=2$, with 3000 probes on each cluster. Both methods converge to the same asymptotic value, with the walker-DBM converging slightly faster.

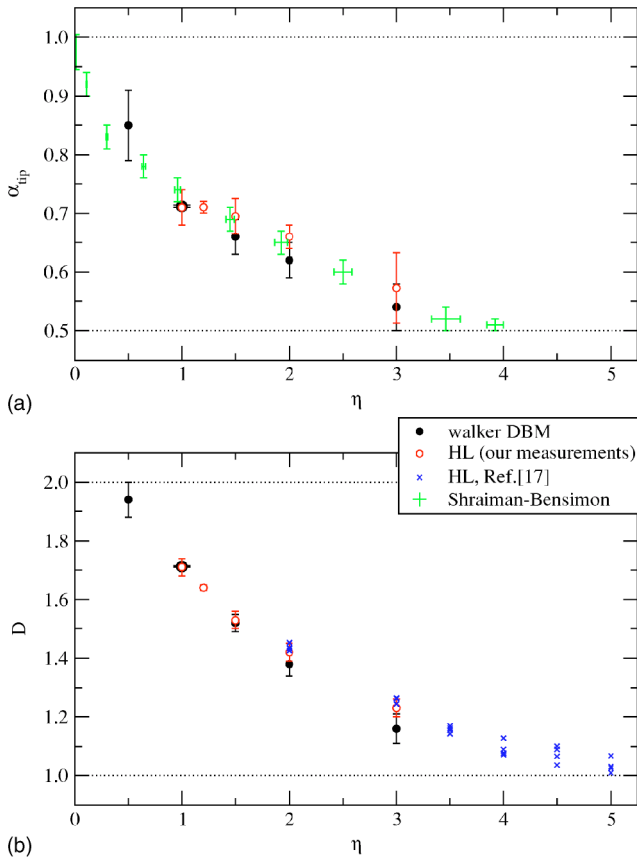


FIG. 8. (Color online) (a) The tip scaling exponent α_{tip} and (b) the fractal dimension D as a function of η . The four data sets plotted are the walker-DBM, our HL measurements, earlier HL measurements of Ref. [17], and our Shraiman-Bensimon results. Because we have to convert the SB results back from measurements at fixed η_1 to the corresponding values of $\eta_0 = \eta_1/\alpha$, these points have error bars on both α and η_0 . The “walker” data point for $\eta = 1$ is in fact a DLA measurement (with very small uncertainties) from Ref. [27] together with the relation $\alpha_{\text{tip}} = D - 1$. The dotted lines correspond to the limiting behaviors: dense two-dimensional growth ($\eta = 0$) and nonbranching one-dimensional growth ($\eta \geq \eta_c$).

scheme. We set the time step adaptively such that for every ψ_k at each time step either the predicted and corrected updates $\delta\psi_k$ agreed within 10% or else ψ_k was being updated by less than 20%. As the predictor-corrector scheme is a second-order method, the resulting worst case error is of order 5%: even this sounds generous but as it was applied to the worst case of 1023 variables the typical precision achieved was very much higher, and we chose 20% on the basis of obtaining results statistically indistinguishable under refinement.

Figure 9(a) shows the observed behavior of $(\sum_{j < k} |\psi_j|^2)^{1/\eta_1}$ versus k with increasing time for a representative value of η_1 . On logarithmic scales the expectation is a straight line with slope $1 - 1/\alpha$ and a difficulty is immediately apparent, in that two-slope behavior is clearly observed. It is clear that it is the slope emerging from lower k values which predominates at large times, although different slope is preserved over a limited upper range of k . Figure 9(b) shows results at long times for various η_1 from which it is clear that while the

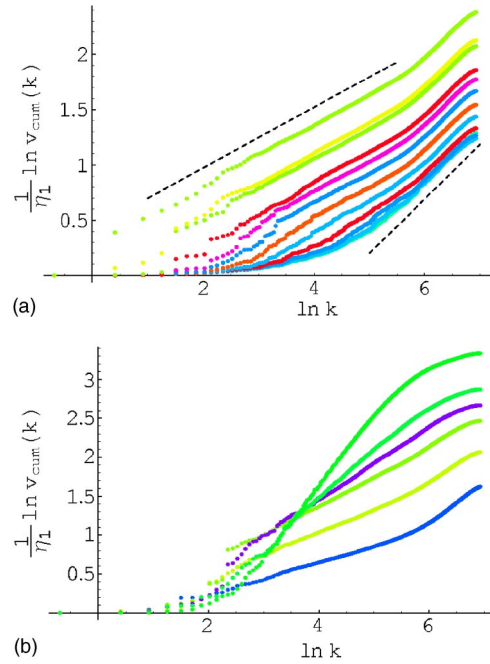


FIG. 9. (Color online) Direct integration of the Bensimon-Shraiman equation (6) as described in Sec. V leads to the prediction that $v_{\text{cum}}(k) = \sum_{j < k} |\psi_j|^2$ should vary as $k^{\eta_1(1-1/\alpha)}$ so the displayed graphs should exhibit slope $1 - 1/\alpha$. (Recall that $\eta_1 = \alpha\eta$.) The upper panel (a) shows plots from the same simulation at $\eta_1 = 0.5$ for successively later-times (bottom to top). There is characteristic slope at high k which persists over a limited range, but it is the lower slope which emerges and eventually dominates the wider range down to the smallest range of k and which we take to reveal the true tip scaling exponent α . The lower panel (b) shows data at large times for $\eta_1 = 0.3, 0.6, 0.9, 1.2, 1.5, 1.8$ (top to bottom at right). While the high- k slope is insensitive to η_1 , there is a clear variation of the asymptotic slopes from which we take α in Fig. 8(a).

high- k slopes are insensitive to η , the (we claim) asymptotic slopes at lower k exhibit a systematic variation.

From the present data the conclusion has to be that the slopes in the lower range of k give our best estimate of $1 - 1/\alpha$ and it is these results which are compared (and agree) with the results by other methods in Fig. 8(a). The relatively constant slopes at high k are what dominated our earlier numerical conclusions in [13,14] which had a factor of 10 less range in k and appeared to lend support to the claim that the slope, and hence α , might be independent of η . That earlier suggestion is clearly refuted, although we cannot rule out more surprises from simulations at decades larger K .

VI. CONCLUSIONS

We have shown that recurrence times between random walkers provide estimates of the local harmonic measure which are highly effective for estimating moments and for simulating nonlinear growth models.

For the scaling of multifractal moments this technique is limited to the regions of the growth which are sufficiently active that nearby hits dominate the screening of a given site, but in that “active range” our results for DLA in two dimen-

sions clearly surpass the quality of previous data and offer more conclusive support to the theoretical exponent relations of Makarov and Halsey. Given that our method is also applicable in higher dimensions, we believe we have established it as the technique of choice to determine harmonic measure in the active range.

Our walker-based simulations of the dielectric breakdown model have greatly consolidated knowledge of how DBM exponents vary with the nonlinearity parameter η in two dimensions. In particular we can now be much more confident of the continuous variation of fractal dimension with η —looking at the trend in terms of α_{tip} sharpens the issue—and we can be fairly confident that the DBM becomes trivial for $\eta > \eta_c = 4$ as conjectured theoretically [16–19].

We have concentrated on measuring exponents relating to the active zone of the growth, which we can determine under growth. Having grown the clusters there is of course no impediment to calculating their full harmonic measure, including screened regions, by more expensive methods applied to a selection of cluster sizes.

The clearest results for the scaling of the DBM in two dimensions over the full range of η now come, ironically,

from our integration of the Shraiman-Bensimon equation. However, unraveling the confusing two-slope behavior which this approach exhibits for the extraction of the exponent α_{tip} would not have been prompted without the walker-DBM results. Overall it is the agreement of both methods with earlier results which establishes the definitive picture.

Finally we note that the most crucial role of walker-based DBM's will be in three dimensions, where the techniques based on complex analysis have nothing to offer and relatively little is known about the exponent behavior. We look forward to exploring this in a subsequent paper.

ACKNOWLEDGMENTS

This research has been supported by the EC under Contract No. HPMF-CT-2000-00800. The computing facilities were provided by the Centre for Scientific Computing of the University of Warwick, with support from the JREI. We thank Joachim Mathiesen and Anders Levermann for providing us with the data of Ref. [25].

-
- [1] T. A. Witten and L. M. Sander, *Phys. Rev. Lett.* **47**, 1400 (1981).
 - [2] R. C. Ball and R. M. Brady, *J. Phys. A* **18**, L809 (1985).
 - [3] S. Tolman and P. Meakin, *Phys. Rev. A* **40**, 428 (1989).
 - [4] J. Nittmann, G. Daccord, and H. E. Stanley, *Nature (London)* **314**, 141 (1985).
 - [5] M. Matsushita, M. Sano, Y. Hayakawa, H. Honjo, and Y. Sawada, *Phys. Rev. Lett.* **53**, 286 (1984).
 - [6] R. M. Brady and R. C. Ball, *Nature (London)* **309**, 225 (1984).
 - [7] E. Somfai, L. M. Sander, and R. C. Ball, *Phys. Rev. Lett.* **83**, 5523 (1999).
 - [8] C. Amitrano, *Phys. Rev. A* **39**, 6618 (1989).
 - [9] R. Ball and M. Blunt, *Phys. Rev. A* **41**, 582 (1990).
 - [10] M. H. Jensen, J. Mathiesen, and I. Procaccia, *Phys. Rev. E* **67**, 042402 (2003).
 - [11] T. C. Halsey, P. Meakin, and I. Procaccia, *Phys. Rev. Lett.* **56**, 854 (1986).
 - [12] L. Niemeyer, L. Pietronero, and H. J. Wiesmann, *Phys. Rev. Lett.* **52**, 1033 (1984).
 - [13] R. C. Ball and E. Somfai, *Phys. Rev. Lett.* **89**, 135503 (2002).
 - [14] R. C. Ball and E. Somfai, *Phys. Rev. E* **67**, 021401 (2003).
 - [15] R. C. Ball, N. E. Bowler, L. M. Sander, and E. Somfai, *Phys. Rev. E* **66**, 026109 (2002).
 - [16] M. B. Hastings, *Phys. Rev. E* **64**, 046104 (2001).
 - [17] M. B. Hastings, *Phys. Rev. Lett.* **87**, 175502 (2001).
 - [18] T. C. Halsey, *Phys. Rev. E* **65**, 021104 (2002).
 - [19] A. Sanchez, F. Guinea, L. M. Sander, V. Hakim, and E. Louis, *Phys. Rev. E* **48**, 1296 (1993).
 - [20] M. B. Hastings and L. S. Levitov, *Physica D* **116**, 244 (1998).
 - [21] B. Shraiman and D. Bensimon, *Phys. Rev. A* **30**, 2840 (1984).
 - [22] T. C. Halsey, M. H. Jensen, L. P. Kadanoff, I. Procaccia, and B. I. Shraiman, *Phys. Rev. A* **33**, 1141 (1986).
 - [23] T. C. Halsey, *Phys. Rev. Lett.* **59**, 2067 (1987).
 - [24] R. C. Ball and O. R. Spivack, *J. Phys. A* **23**, 5295 (1990).
 - [25] M. H. Jensen, A. Levermann, J. Mathiesen, and I. Procaccia, *Phys. Rev. E* **65**, 046109 (2002).
 - [26] N. G. Makarov, *Proc. London Math. Soc.* **51**, 369 (1985).
 - [27] E. Somfai, R. C. Ball, J. P. DeVita, and L. M. Sander, *Phys. Rev. E* **68**, 020401 (2003).